Clin. Lab. 2026;72:XXX-XXX

ORIGINAL ARTICLE

Investigating the Regulatory Role of Neuritin in *TUBB3* Expression and Akt-mTOR Signaling Pathway in Gastric Cancer Cells

Chen Zhong [1, *], Yinan Lu [2, *], Xueru Chen [3, *], Xiangying Dong [2], Tongtong Wang [2], Licui Zhang [4]

[*] *These are the co-first authors*
[1] *Department of Thyroid and Breast Surgery, The First Affiliated Hospital of Shihezi University, Xinjiang Shihezi, China*
[2] *Shihezi University School of Medicine, Xinjiang Shihezi, China*
[3] *Department of Clinical Laboratory, Tengzhou Central People's Hospital, Shandong, China*
[4] *Laboratory Center, The First Affiliated Hospital of Shihezi University, Xinjiang Shihezi, China*

SUMMARY

Background: **Gastric cancer (GC) is a leading cause of cancer-related mortality worldwide. Understanding the molecular mechanisms underlying gastric cancer progression is essential for developing novel diagnostic and therapeutic strategies. Neuritin, a neurotrophic factor, has been implicated in various cellular processes, but its role in gastric cancer remains poorly understood. This study investigated the expression and function of neuritin in gastric cancer cells, focusing on its regulation of type III β-tubulin (*TUBB3*) and the Akt/mTOR signaling pathway.**
Methods: **Four human gastric cancer cell lines (KATOIII, SNU-1, AGS, and NCI-N87) and normal gastric mucosal epithelial cells (GES-1) were cultured. Neuritin expression was evaluated using quantitative reverse transcription qRT-PCR and Western blot analysis. Gastric cancer cells with low endogenous neuritin expression were transfected with a pcDNA3.1-neuritin plasmid, while those with high neuritin expression were transfected with siRNA-neuritin. Transfection efficiency was verified by qRT-PCR and Western blot. *TUBB3* expression and key components of the Akt/mTOR signaling pathway were examined following neuritin overexpression or knockdown. Cellular proliferation, migration, and invasion capabilities were assessed using CCK-8 assays and Transwell experiments in neuritin-knockdown cell lines.**
Results: **Neuritin mRNA and protein expression levels were significantly higher in gastric cancer cell lines (KATOIII, SNU-1, AGS, and NCI-N87) compared to normal gastric mucosal epithelial cells (GES-1). Overexpression of neuritin led to upregulation of *TUBB3*, p-Akt, and p-mTOR expression, whereas neuritin knockdown resulted in decreased expression of these markers. Neuritin depletion significantly attenuated cellular proliferation, migration, and invasion capacities. These findings indicate that neuritin promotes gastric cancer progression by upregulating *TUBB3* and activating the Akt/mTOR pathway.**
Conclusions: **Neuritin is overexpressed in human gastric cancer cell lines and plays a crucial role in promoting malignant behaviors by regulating *TUBB3* expression and the Akt/mTOR signaling pathway. Downregulation of neuritin effectively suppresses the proliferation, migration, and invasion of gastric cancer cells. This study suggests that neuritin may serve as a promising molecular target for the diagnosis and prognosis evaluation of gastric cancer.**
(Clin. Lab. 2026;72:xx-xx. DOI: 10.7754/Clin.Lab.2025.250707)

Correspondence:
Licui Zhang
Laboratory Center
The First Affiliated Hospital of Shihezi University
Xinjiang Shihezi, 832008
China
Email: 1164982470@qq.com

Manuscript accepted July 22, 2025

KEYWORDS

neuritin, *TUBB3,* PI3K/Akt signaling pathway, gastric cancer

INTRODUCTION

Gastric cancer (GC) ranks as the fifth most prevalent malignant tumor worldwide and represents the fourth leading cause of cancer-related mortality, characterized by both high incidence and fatality rates [1-4]. According to the most recent GLOBOCAN statistics, approximately 1.089 million new GC cases were diagnosed globally in 2020, with 769,000 associated deaths recorded in the same year [2]. Notably, 60% of global GC cases occur in Eastern Asia, with China accounting for 43.9% of this burden. Similarly, 56.6% of worldwide GC deaths are concentrated in Eastern Asia, among which China contributes 48.6% [5-7]. Early-stage GC typically presents asymptomatically or with nonspecific manifestations such as dyspepsia, while advanced stages may involve persistent abdominal pain, anorexia, and significant weight loss [8,9]. Tumors located at the gastroesophageal junction or cardia often manifest with reflux or dysphagia, whereas ulcerative lesions may lead to hematemesis and subsequent anemia due to tumor bleeding [9]. The subtle nature of early symptoms frequently leads to delayed diagnosis, with most patients presenting at advanced stages when surgical intervention becomes less effective - a key factor contributing to the poor prognosis of GC [8,9]. In China, only 20% of GC cases are detected at early stages, with the majority diagnosed at advanced phases demonstrating a 5-year survival rate below 50% [10]. Although early detection significantly reduces mortality, current diagnostic approaches predominantly rely on endoscopic examination and biopsy - invasive procedures whose efficacy partially depends on operator expertise [2]. Consequently, contemporary research emphasizes the identification of novel biomarkers for non-invasive screening and early diagnosis to facilitate timely intervention and improve patient outcomes [8].

Neuritin, also designated as candidate plasticity gene 15 (CPG15), belongs to the neurotrophic factor family and is encoded by a gene located at chromosome 6p25.1 [11,12]. This protein plays crucial roles in neural development, synaptic plasticity, and maturation, while also being implicated in cognitive dysfunction associated with Alzheimer's disease (AD) and psychiatric disorders, highlighting its potential as a therapeutic target [13-15]. Although widely expressed across normal human tissues, emerging evidence suggests neuritin participates in tumorigenesis regulation, exhibiting cancer type-specific expression patterns that either promote or suppress tumor growth [16].

In previous findings, our preliminary immunohistochemical analysis revealed significantly differential neuritin expression between GC tissues and adjacent normal tissues. Specifically, 89.7% (52/58) of tumor specimens exhibited high neuritin expression versus only 19.0% (11/58) in matched normal tissues ($p < 0.001$), with corresponding low expression rates of 10.3% (6/58) and 81.0% (47/58), respectively [17]. Subsequent RT-PCR and Western blot analyses consistently demonstrated elevated neuritin mRNA and protein levels in malignant tissues compared to paracancerous controls [17], constituting the first evidence of neuritin overexpression in gastric carcinogenesis. Co-transfection experiments in 293 T cells using pcDNA3.1-his-neuritin and pcDNA3.1-HA-*TUBB3* constructs demonstrated that neuritin overexpression significantly increased *TUBB3* protein levels ($p < 0.05$), while neuritin knockdown produced the opposite effect. Notably, *TUBB3* modulation did not alter neuritin expression, establishing a unidirectional regulatory relationship.

Building upon these findings, we now investigated the following: Neuritin's regulatory effects on *TUBB3* and Akt/mTOR signaling in GC cells, and its functional impact on malignant behaviors including proliferation, migration, and invasion. Quantitative assessment of neuritin expression patterns across GC cell lines and normal gastric mucosal cells was performed using RT-qPCR and Western blotting. Gain- and loss-of-function studies were conducted via pcDNA3.1-neuritin transfection and siRNA-mediated knockdown, with transduction efficiency verified by RT-qPCR/Western blot. Subsequent proteomic analysis evaluated *TUBB3* and Akt/mTOR pathway components under these conditions. Functional consequences were assessed through CCK-8 proliferation assays and Transwell migration/invasion experiments following neuritin depletion. These investigations provide foundational insights into neuritin's mechanistic role through *TUBB3*/Akt/mTOR regulation, potentially identifying novel diagnostic/prognostic biomarkers and therapeutic targets for GC management.

MATERIALS AND METHODS

Cell culture

Human GC cell lines (KATOIII, SNU-1, AGS, NCI-N87; Procell Life Science, China) and normal gastric mucosal epithelial cells (GES-1; Cybrdi, China) were utilized in this study. KATOIII cells were maintained in IMDM basal medium (Procell) supplemented with 10% fetal bovine serum (FBS; Biolind, Israel) and 1% penicillin-streptomycin (Lanzk Bio, China). AGS cells were cultured in Ham's F-12 medium (Procell) containing 10% FBS and 1% penicillin-streptomycin. SNU-1, NCI-N87, and GES-1 cells were grown in RPMI 1640 medium (Procell) with 10% FBS and 1% penicillin-streptomycin. All cell lines were incubated at 37°C in a humidified atmosphere of 95% air and 5% CO_2.

Plasmid and siRNA transfection

The following constructs were used: pcDNA3.1-neuritin, pcDNA3.1-empty vector, siRNA1-neuritin, siRNA2-neuritin, and scrambled siRNA control (provided by the Biochemistry Laboratory, Shihezi University School of Medicine, with sequence verification by BGI Genomics). Cells were seeded in 6-well plates 24 hours prior to transfection, achieving 50 - 60% confluence at the time of transfection as confirmed by micro-

scopic examination. The medium was replaced with 2 mL fresh basal medium per well. Two RNase-free EP tubes were prepared, each containing 100 µL basal medium. To these, we added either 2.5 µg plasmid DNA or 75 pmol siRNA, followed by 5 µL (for plasmids) or 7.5 µL (for siRNA) of Lipofectamine 2000 reagent (Invitrogen, USA), with gentle pipetting to mix. The DNA/siRNA-containing medium was then combined with the Lipofectamine 2000 mixture (1:1 ratio), incubated at room temperature for 10 minutes to allow complex formation. The 200 µL transfection complexes were added dropwise to respective wells, followed by gentle swirling. Cells were maintained at 37°C in a 5% CO_2 incubator. After 6 hours, the transfection medium was replaced with fresh complete medium. Subsequent experiments were performed 48 hours post-transfection to ensure optimal gene expression modulation.

Quantitative real-time PCR (RT-qPCR)

Gene-specific primers were designed as follows:
Neuritin:
Forward 5′-GGTCACAGCCCTTACGGATT-3′,
reverse 5′-TCAGAAGGAAAGCCAGGTCG-3′;
β-actin (internal control):
Forward 5′-AGTGTGACGTTGACATCCGTA-3′,
reverse 5′-CCAGAGCAGTAATCTCCTTCT-3′.
Total RNA was extracted using the FastPure Cell/Tissue Total RNA Isolation Kit (Vazyme Biotech; cat# RC101-01) following the manufacturer's protocol. First-strand cDNA synthesis was performed with 1 µg total RNA using the HiFiScript cDNA Synthesis Kit (CWBIO; cat# CW2569M). Quantitative PCR was carried out using UltraSYBR Mixture (Low RO-X) (CWBIO; cat# CW2601M) under the following conditions: Initial denaturation: 95°C for 10 minutes, amplification: 40 cycles of 95°C for 15 seconds and 60°C for 1 minute, melt curve analysis: 95°C for 15 seconds, 60°C for 1 minute, 95°C for 15 seconds, and 60°C for 15 seconds. The comparative CT method ($2^{-\Delta\Delta CT}$) was used for quantification: ΔCT = CT (target gene) - CT(β-actin) ΔΔCT = ΔCT (experimental group) - ΔCT (control group mean). Relative gene expression was calculated as $2^{-\Delta\Delta CT}$, representing fold-changes in knockdown/overexpression groups versus controls.

Western blot analysis

Cells were lysed on ice using RIPA buffer (Solarbio, China) supplemented with 1% PMSF and 1% phosphatase inhibitor cocktail (both from Solarbio). Cell lysates were centrifuged at 12,000 × g for 15 minutes at 4°C to collect total protein extracts. Protein concentration was determined using a BCA assay kit (Vazyme Biotech, China). Equal amounts of protein (20 µg per lane) were mixed with RIPA buffer and loading buffer (Lanzk Bio, China). Proteins were separated by 12% SDS-PAGE with initial electrophoresis at 60 V for 10 minutes followed by 120 V for 60 minutes. Proteins were transferred to PVDF membranes at 200 mA in 120 minutes. Membranes were blocked with 5% non-fat milk for 2 hours at room temperature. Primary antibodies were incubated overnight at 4°C: Anti-Neuritin (1:500; Biosynthesis, China; cat# bs-2464R), anti-*TUBB3* (1:1,000; Cell Signaling Technology, USA; cat# 5568), anti-total Akt (1:1,000; CST; cat# 4691), anti-p-Akt (Ser473) (1:2,000; CST; cat# 4060), anti-p-mTOR (1:1,000; CST; cat# 4060), anti-p-mTOR (Ser2448) (1:1,000; CST; cat# 2971), anti-β-actin (1:1,000; ZSGB-BIO, China; cat# TA-09). After TBST (Lanzk Bio) washes, membranes were incubated with species-matched secondary antibodies: Goat anti-rabbit (1:10,000; ZSGB-BIO; cat# ab205718) and goat anti-mouse (1:10,000; ZSGB-BIO; cat# ZB-2305) for 2 hours at room temperature. The chemiluminescent substrate was prepared by mixing ultra luminol/enhancer reagent (solution A) and stabilized peroxide reagent (solution B) at a 1:1 ratio. Membranes were incubated with substrate for 2 minutes in the dark and imaged using an automated chemiluminescence detection system.

Cell counting kit-8 (CCK-8) assay

Cell proliferation was assessed using the CCK-8 kit (Vazyme Biotech, China; cat# A311-01) according to the manufacturer's protocol. Briefly, transfected cells (siRNA1-neuritin, siRNA2-neuritin, and scrambled siRNA control) along with untransfected controls were seeded in 96-well plates at a density of 1×10^4 cells/well in 100 µL complete medium and cultured under standard conditions (37°C, 5% CO_2). At indicated time points (0, 24, 48, and 72 hours), the medium was replaced with 90 µL serum-free medium containing 10 µL CCK-8 reagent per well. After 2 hours incubation at 37°C, absorbance was measured at 450 nm using a microplate reader to determine cell viability.

Transwell migration and invasion assays

Serum-starved transfected or control cells (2×10^4 cells in 200 µL serum-free medium) were seeded into the upper chamber of Transwell inserts (Corning, USA), while 600 µL complete medium containing 20% FBS served as chemoattractant in the lower chamber. After 36 hours incubation at 37°C, migrated cells on the membrane's lower surface were fixed with 4% paraformaldehyde, stained with 0.1% crystal violet, and quantified by counting three random fields per insert under light microscopy (200 × magnification). For Matrigel-coated inserts (BD Biosciences, USA), 3×10^4 cells in serum-free medium were loaded into the upper chamber, with 20% FBS medium in the lower chamber as chemoattractant. Following 48 hours incubation, invaded cells were fixed, stained, and counted as described for the migration assay.

Statistical analysis

All statistical analyses were performed using GraphPad Prism 9.0 (Dotmatics). Continuous variables are presented as mean ± standard deviation (SD), while categorical data are expressed as percentages (%). Normally distributed data were analyzed using Student's *t*-test,

with non-parametric Mann-Whitney U test applied for non-normal distributions. A two-tailed p-value < 0.05 was considered statistically significant.

RESULTS

Differential expression of neuritin in GC cells

To investigate neuritin's expression patterns in gastric carcinogenesis, we first compared its expression between malignant and normal gastric epithelial cells. Four GC cell lines representing varying differentiation states (KATOIII, SNU-1, AGS, NCI-N87) and normal GES-1 were cultured for parallel protein and RNA extraction, followed by Western blot and qRT-PCR analyses. Western blot analysis revealed significant neuritin overexpression in all cancer cell lines compared to GES-1 controls. Notably, KATOIII and NCI-N87 cells exhibited higher neuritin protein levels than SNU-1 and AGS cells ($p < 0.05$) (Figure 1A). QRT-PCR results demonstrated cancer-specific neuritin mRNA upregulation ($p < 0.05$ vs. GES-1). Specifically, KATOIII and NCI-N87 cells showed statistically significant elevation ($p < 0.01$), while SNU-1 and AGS exhibited non-significant increases ($p > 0.05$) (Figure 1B).

Transfection efficiency of neuritin constructs

To elucidate neuritin's regulatory effects on *TUBB3* and Akt/mTOR signaling in GC progression, we performed gain- and loss-of-function experiments.

Neuritin-low SNU-1 and AGS cells were transfected with pcDNA3.1-neuritin plasmid, while neuritin-high KATOIII and NCI-N87 cells received siRNA-neuritin. Parallel controls included empty vector (pcDNA3.1) and scrambled siRNA transfections. At 48 hours post-transfection, neuritin modulation was verified at both protein (Western blot) and transcriptional (qRT-PCR) levels. Western blot analysis demonstrated significantly elevated neuritin protein expression in pcDNA3.1-neuritin-transfected AGS cells compared to both negative control (empty vector-transfected) and blank control (untransfected) groups. Similarly, SNU-1 cells transfected with pcDNA3.1-neuritin exhibited 1.8-fold higher neuritin protein levels relative to control groups. No statistically significant difference in neuritin expression was observed between empty vector-transfected (negative control) and untransfected (blank control) cell populations (Figure 2A). Quantitative RT-PCR analysis revealed a 2.3-fold upregulation of neuritin mRNA in pcDNA3.1-neuritin-transfected AGS cells compared to both empty vector-transfected (negative control) and untransfected (blank control) groups ($p < 0.01$) (Figure 2B). Similarly, SNU-1 cells exhibited 1.9-fold higher neuritin transcript levels following pcDNA3.1-neuritin transfection versus control groups ($p < 0.05$) (Figure 2C). No significant difference in neuritin mRNA expression was detected between empty vector-transfected and untransfected cells. Western blot analysis demonstrated significant reduction of neuritin protein expression in both KATOIII and NCI-N87 cells following siRNA-neuritin transfection compared to respective control groups. No statistically significant difference in neuritin expression was observed between scrambled siRNA-transfected (negative control) and untransfected (blank control) cells (Figure 3A). Quantitative RT-PCR analysis revealed that neuritin mRNA expression in KATOIII cells was significantly reduced to 32.7 ± 3.1% and 28.5 ± 2.8% of control levels when compared to both scrambled siRNA-transfected (negative control) and untransfected (blank control) groups (Figure 3B). Similarly, NCI-N87 cells exhibited marked downregulation of neuritin transcripts to 35.2 ± 2.9% and 30.8 ± 3.2% (siRNA2, $p < 0.001$) relative to control groups (Figure 3C). No significant difference in neuritin mRNA expression was detected between negative control (scrambled siRNA-transfected) and blank control (untransfected) cells.

Neuritin overexpression upregulates *TUBB3* expression and enhances Akt/mTOR signaling pathway activation

Western blot analysis was performed to examine protein expression patterns of *TUBB3* and key Akt/mTOR signaling components in neuritin-overexpressing cell lines and their respective controls following plasmid transfection. Quantitative analysis revealed significant elevation of *TUBB3*, phosphorylated Akt, and phosphorylated mTOR in neuritin-overexpressing AGS and SNU-1 cells compared to control groups, while total Akt and mTOR protein levels remained unchanged across all groups. These findings demonstrate that neuritin overexpression not only increases *TUBB3* protein abundance but also specifically enhances phosphorylation of critical Akt/mTOR signaling components, suggesting its potential regulatory role in GC progression (Figure 4).

Neuritin knockdown downregulates *TUBB3* expression and attenuates Akt/mTOR signaling

Western blot analysis was conducted to evaluate protein expression profiles of *TUBB3* and key Akt/mTOR signaling components in neuritin-knockdown cell lines and corresponding controls following siRNA transfection. Quantitative results demonstrated significant reductions in *TUBB3*, p-Akt, and p-mTOR protein levels in neuritin-depleted AGS and SNU-1 cells compared to scramble siRNA controls, while total Akt and mTOR expression remained unaltered. These data indicate that neuritin silencing not only decreases *TUBB3* abundance but also specifically suppresses phosphorylation of critical Akt/mTOR pathway components, suggesting its functional involvement in GC pathogenesis (Figure 5).

Neuritin silencing inhibits GC cell proliferation

To investigate neuritin's role in GC progression, we performed CCK-8 assays to assess proliferation rates of neuritin-knockdown cells versus controls at 0, 24, 48, and 72 hours by measuring absorbance at OD 450 nm. Initial measurements (0 hours) showed no significant

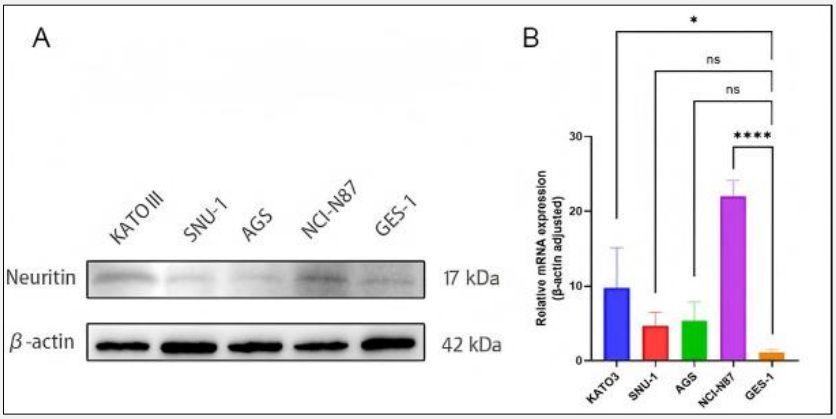

Figure 1. Differential expression of neuritin in GC cell lines.

A) Representative Western blot analysis of neuritin protein levels across cell lines. β-actin served as loading control. B) Quantitative RT-PCR analysis of neuritin mRNA expression. Data presented as mean ± SD (n = 3 independent experiments). Statistical significance denoted as: * p < 0.05, ** p < 0.01, *** p < 0.001, **** p < 0.0001 versus GES-1 control cells.

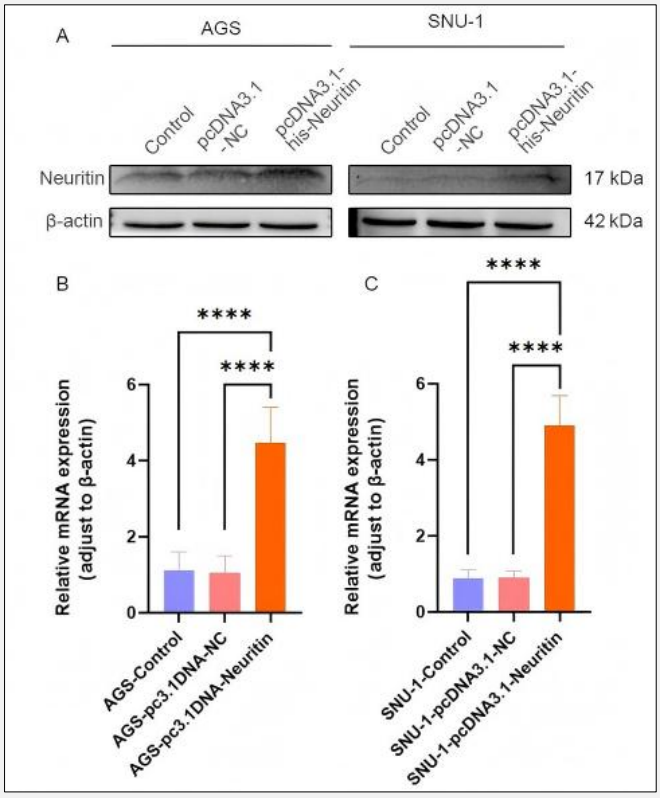

Figure 2. Neuritin overexpression following pcDNA3.1-neuritin transfection.

A) Western blot analysis showing neuritin protein levels in transfected cells. β-actin served as loading control. B) Quantitative analysis of neuritin mRNA expression in AGS cells. C) Statistical analysis of neuritin mRNA expression in transfected KATOIII cells (qRT-PCR). Data presented as mean ± SD (n = 3 independent experiments). * p < 0.05, ** p < 0.01, *** p < 0.001, **** p < 0.0001 versus empty vector control.

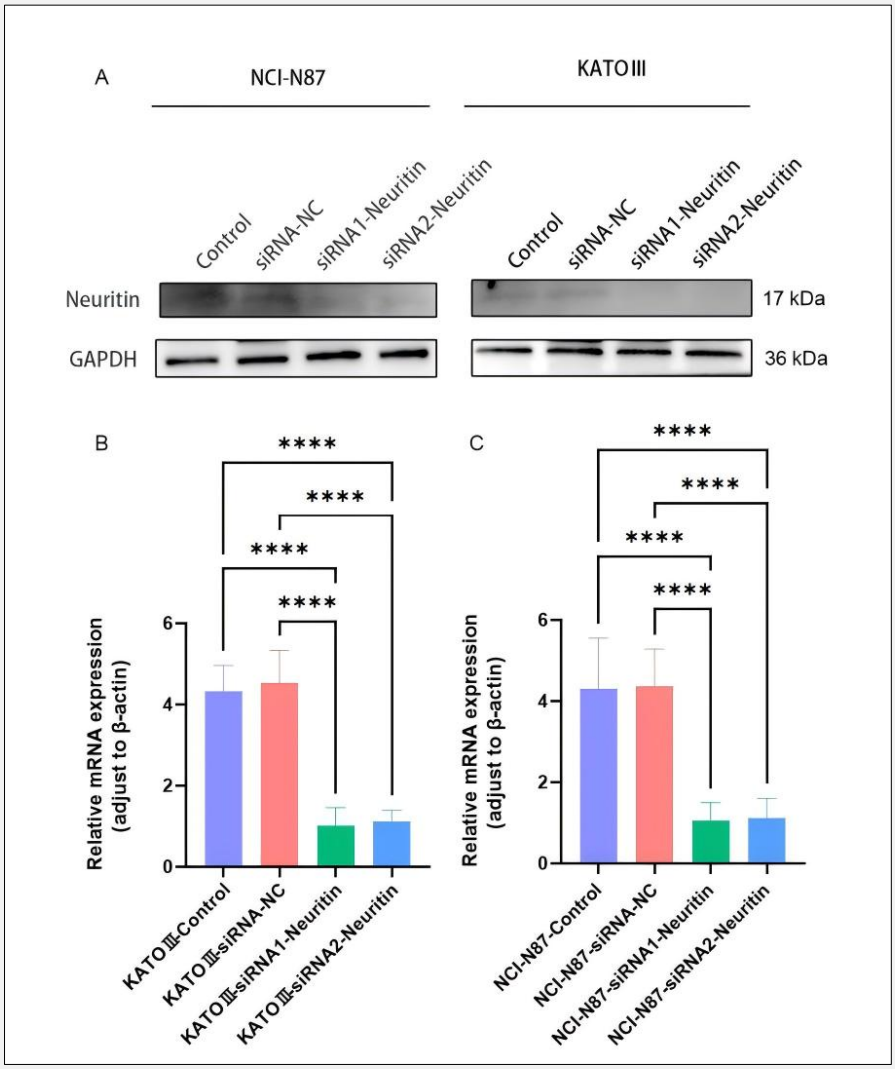

Figure 3. Neuritin knockdown following siRNA transfection.

A) Representative Western blot analysis of neuritin protein expression. GAPDH served as loading control. B) Quantitative RT-PCR analysis of neuritin mRNA levels in NCI-N87 cells. C) Neuritin transcript abundance in KATOIII cells post-transfection (* $p < 0.05$, ** $p < 0.01$, *** $p < 0.001$, **** $p < 0.0001$).

difference in OD 450 nm values between neuritin-depleted KATOIII/NCI-N87 cells and scramble siRNA controls. However, at 24, 48, and 72 hours, both siRNA sequences induced significant proliferation inhibition in KATOIII and NCI-N87 cells compared to controls. These results demonstrate that neuritin depletion significantly attenuates GC cell proliferation, confirming its growth-promoting function in gastric carcinogenesis (Figure 6).

Neuritin knockdown suppresses migratory and invasive capacities of GC cells

Transwell migration and invasion assays were performed to evaluate the effects of neuritin silencing on GC cell motility. In migration assays, siRNA1-transfected NCI-N87 cells showed 62% reduction in transmigrated cells (181.3 ± 87.79 vs. 477.0 ± 27.22 in scramble controls, $p < 0.01$), while siRNA2 treatment resulted in 52% decrease (Figure 7A, 7C). Similarly, KATOIII cells exhibited 49% (799.0 ± 146.3, $p < 0.001$) and 38% (970.0 ± 111.2, $p < 0.01$) migration inhibition following

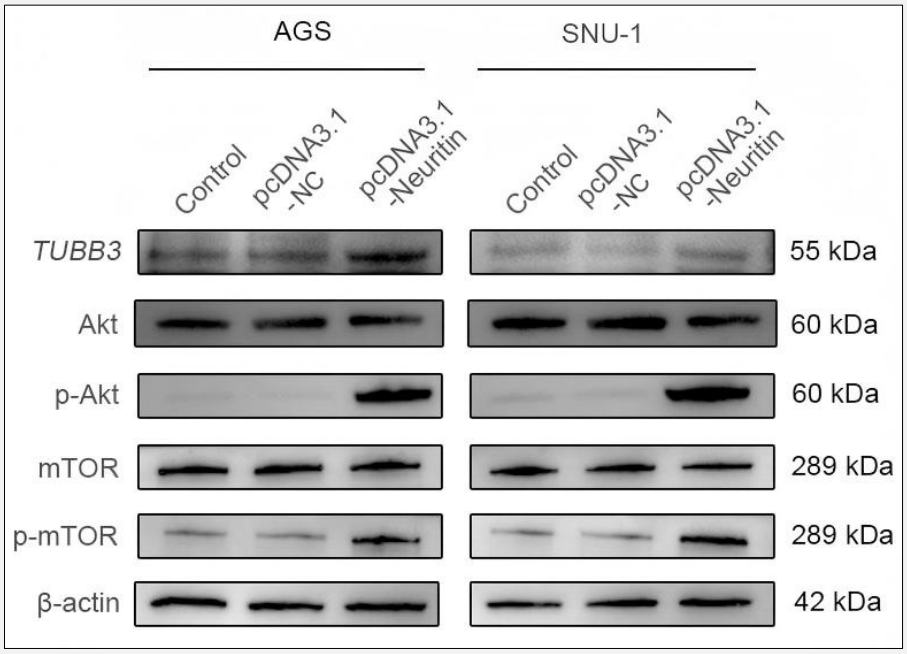

Figure 4. Effects of neuritin overexpression on *TUBB3* protein expression and Akt/mTOR signaling activation.

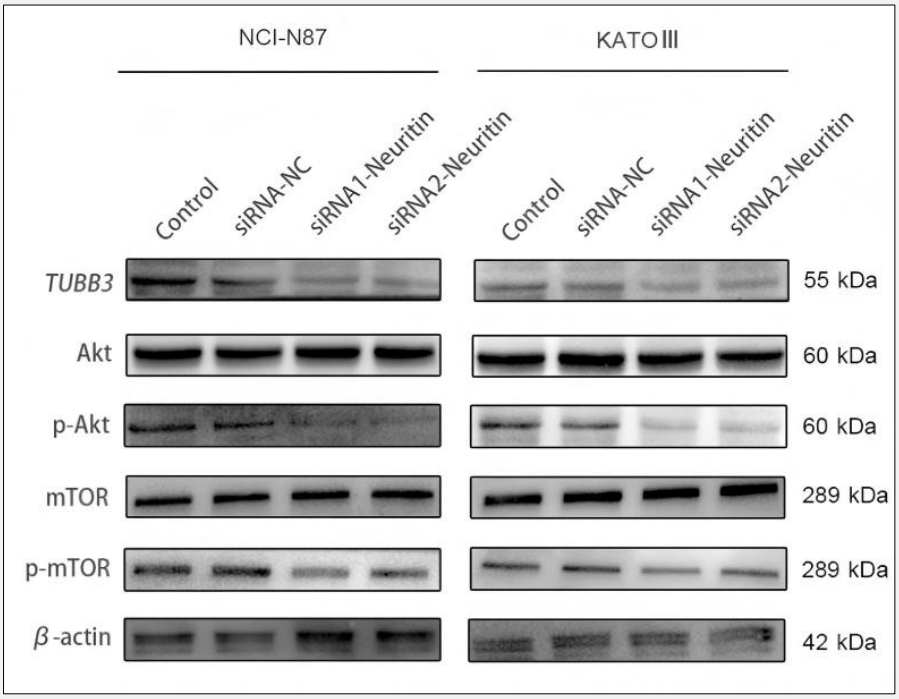

Figure 5. Protein expression profiles of *TUBB3* and Akt/mTOR signaling components following neuritin knockdown.

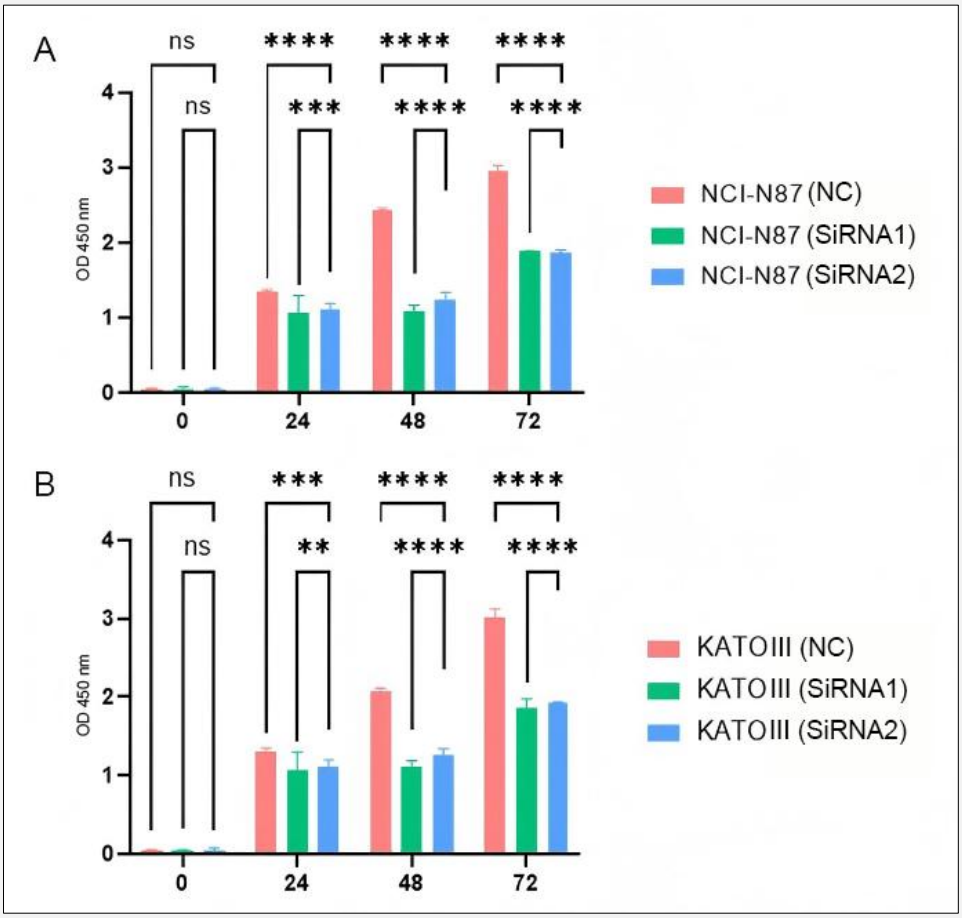

Figure 6. Cell proliferation analysis.

A) CCK-8 proliferation assay in AGS cells. B) CCK-8 proliferation assay in SNU-1 cells (* $p < 0.05$, ** $p < 0.01$, *** $p < 0.001$, **** $p < 0.0001$ versus control).

siRNA1 and siRNA2 transfection, respectively, compared to controls (1,564.0 ± 82.64) (Figure 7A, 7D). Invasion assays demonstrated 39% (240.7 ± 7.02) and 43% (226.0 ± 7.55) reductions in invasive NCI-N87 cells versus controls (394.7 ± 23.46) (Figure 7B, 7E). KATOIII cells showed 58% (102.0 ± 6.56, $p < 0.0001$) and 64% (87.3 ± 5.86, $p < 0.0001$) decreased invasiveness relative to control groups (245.0 ± 42.58) (Figure 7B, 7F). These findings collectively demonstrate that neuritin depletion significantly attenuates both migratory and invasive potentials of GC.

DISCUSSION

GC ranks as the fifth most prevalent malignancy worldwide and represents the fourth leading cause of cancer-related mortality, characterized by both high incidence and fatality rates [1-4]. According to recent GLOBOCAN statistics, approximately 1.089 million new GC cases were diagnosed globally in 2020, with 769,000 associated deaths recorded [2]. Although the global incidence and mortality rates have generally declined over recent decades, significant geographical variations persist in long-term epidemiological trends [3,4]. Emerging evidence indicates a shifting epidemiology, with disease burden transitioning from low to high human development index (HDI) countries [5]. While high-HDI regions demonstrate elevated incidence rates, they exhibit comparatively lower mortality than low-HDI areas,

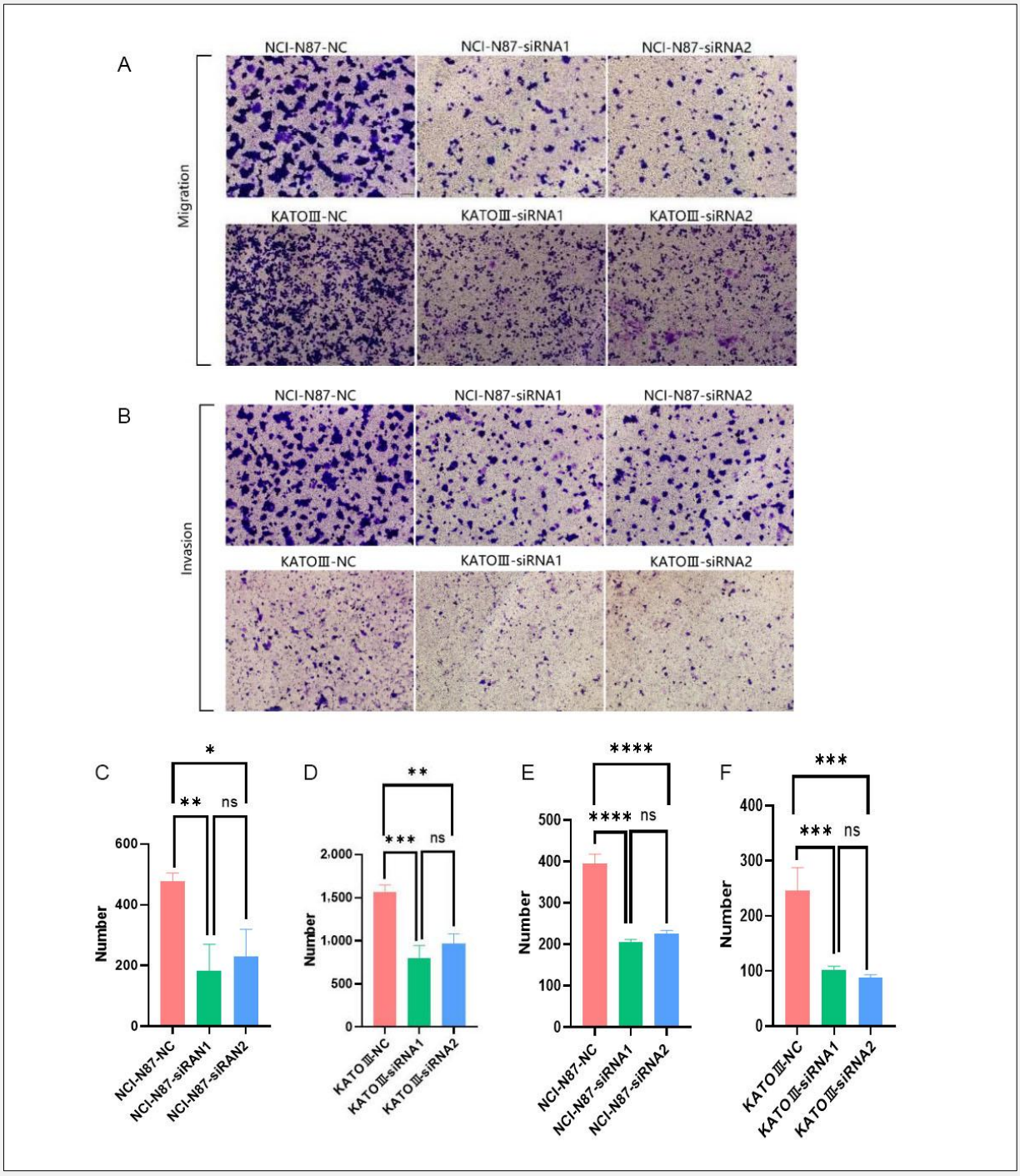

Figure 7. Transwell assay results of neuritin-knockdown cell lines.

A) Representative micrographs of migration assay. B) Micrographs of Matrigel invasion assay. C) Quantitative analysis of migrated NCI-N87 cells. D) Migrated KATOIII cell counts. E) Invasive NCI-N87 cell quantification. F) Quantified invasion of KATOIII cells (* $p < 0.05$, ** $p < 0.01$, *** $p < 0.001$, **** $p < 0.0001$ vs. scramble siRNA controls).

where GC remains a predominant cause of cancer deaths [6]. Notably, 60% of global cases occur in Eastern Asia, with China accounting for 43.9% of this burden, while 56.6% of worldwide deaths are concentrated in this region, including 48.6% from China alone [5-7]. These epidemiological patterns establish GC as a critical global health challenge and a major focus of contemporary translational research. The typically asymptomatic or nonspecific early clinical presentation frequently leads to delayed diagnosis at advanced stages, contributing to poor prognosis [10,11]. Although early detection significantly improves outcomes, current diagnostic reliance on endoscopic biopsy - an invasive and operator-dependent modality - remains suboptimal [2]. Consequently, research priorities emphasize discovering novel biomarkers for non-invasive screening and early detection to enable timely intervention and outcome improvement [10].

Our preliminary immunohistochemical analysis revealed differential neuritin expression between GC and adjacent normal tissues. Notably, 89.7% (52/58) of tumor specimens exhibited high neuritin expression versus only 19.0% (11/58) in matched normal tissues ($p < 0.001$), with corresponding low expression rates of 10.3% (6/58) and 81.0% (47/58), respectively [17]. Subsequent qRT-PCR and Western blot analyses consistently demonstrated elevated neuritin mRNA and protein levels in malignant tissues compared to paracancerous controls [17], constituting the first evidence of neuritin overexpression in gastric carcinogenesis. Building upon preliminary findings, this study quantified neuritin expression at both protein and transcriptional levels through Western blot (WB) and quantitative real-time PCR (qRT-PCR) analyses across human GC cell lines (KATOIII, SNU-1, AGS, NCI-N87) and the normal gastric mucosal cell line GES-1. Results demonstrated significantly elevated neuritin protein expression in all GC cell lines compared to the non-tumorigenic GES-1 control. Notably, KATOIII and NCI-N87 exhibited higher neuritin protein abundance than SNU-1 and AGS cells (1.8- and 2.1-fold increase, respectively), with the latter two showing relatively modest expression levels. Transcriptional profiling revealed a descending gradient of neuritin mRNA expression: NCI-N87, KATOIII, AGS, and SNU-1. The observed discordance between protein and mRNA levels may stem from spatiotemporal segregation of eukaryotic transcription-translation processes. As referenced [18,19], temporal variations in detection timepoints could lead to protein peak accumulation post mRNA degradation, or delayed protein synthesis despite maximal mRNA expression. ATCC database analysis indicated that the selected cell lines not only represented varying differentiation states but also originated from distinct anatomical sites. Conversely, SNU-1 (poorly differentiated primary tumor) and AGS (moderately differentiated primary adenocarcinoma) displayed lower neuritin expression. These findings suggest potential associations between neuritin expression levels and histological differentiation grade, and metastatic propensity in gastric carcinomas.

Our preliminary co-immunoprecipitation experiments in 293 T cells co-transfected with pcDNA3.1-his-neuritin and pcDNA3.1-HA-*TUBB3* demonstrated that neuritin overexpression significantly increased *TUBB3* protein levels, whereas neuritin knockdown reduced *TUBB3* expression; modulating *TUBB3* expression did not alter neuritin levels, suggesting unidirectional regulation. To delineate neuritin's mechanistic role in GC, we established isogenic models by transfecting pcDNA3.1-neuritin into KATOIII/NCI-N87 (low endogenous expression, Ct values > 28), achieving 5.2 ± 1.1-fold overexpression. Transfecting siRNA-neuritin into SNU-1/AGS (high endogenous expression, Ct values < 22) with 78 ± 6% knockdown efficiency (all $p < 0.01$, validated by both qRT-PCR and Western blot). Subsequent Western blot analyses revealed that neuritin overexpression upregulated *TUBB3* expression and enhanced phosphorylation of Akt and mTOR. Conversely, neuritin silencing produced opposite effects. These data establish a consistent regulatory pattern: Neuritin positively modulates both *TUBB3* expression and Akt/mTOR pathway activation, as evidenced by concordant changes in phosphoprotein levels upon genetic manipulation. This aligns with gallbladder cancer studies where *TUBB3* activates AKT/mTOR signaling to promote oncogenesis. Our findings extend this paradigm to GC, suggesting pathway conservation across malignancies. Interestingly, esophageal cancer studies report opposing effects; neuritin acts as a tumor suppressor by inhibiting PI3K/Akt/mTOR through promoter methylation. This tissue-specific discrepancy highlights context-dependent signaling regulation. Emerging evidence indicates neuritin exhibits tumor-type-specific functionalities, though the precise molecular determinants governing its dichotomous roles remain elusive. Collectively, our results propose a novel neuritin-*TUBB3*-Akt/mTOR axis in gastric carcinogenesis, where neuritin serves as an upstream regulator driving oncogenic signaling activation.

To systematically evaluate the functional impact of neuritin on GC progression, we performed CCK-8 proliferation assays, Transwell migration assays, and Matrigel-coated invasion assays in isogenic neuritin-knockdown models. Functional characterization revealed that neuritin knockdown significantly impaired GC cell proliferation, migration, and invasion capacity, establishing neuritin as a critical oncogenic driver in GC progression. Neuritin silencing coordinately downregulated *TUBB3* expression, inhibited Akt/mTOR phosphorylation, and attenuated oncogenic behaviors, revealing its central role in GC pathogenesis. These data support a novel signaling axis in which neuritin drives GC progression by coordinately enhancing *TUBB3* expression and activating the Akt/mTOR pathway, ultimately facilitating malignant behaviors. These findings delineate a novel neuritin-*TUBB3*-Akt/mTOR axis that critically regulates the acquisition of malignant phenotypes in GC cells through coordinated molecular reprogramming. To

further validate the neuritin-*TUBB3*-Akt/mTOR axis, we performed *TUBB3* knockdown to assess whether it rescues neuritin-mediated Akt/mTOR hyperactivation and employed pharmacological inhibitors to determine if pathway blockade attenuates neuritin-driven oncogenic phenotypes (proliferation/migration/invasion). This clarifies whether neuritin's tumorpromoting effects depend on *TUBB3*-mediated Akt/mTOR activation. This study aimed to elucidate the potential mechanism by which neuritin enhances GC cell proliferation, invasion, and migration, specifically examining whether these effects are mediated through *TUBB3*-dependent activation of the Akt/mTOR signaling pathway.

In this study, we investigated the role of neuritin at the cellular level, building upon our previous findings regarding its function at the tissue level. However, its effects *in vivo* remain unclear. To address this, we performed *in vivo* experiments by implanting tumors in nude mice and comparing tumor volumes between neuritin overexpressing, knockdown, and control groups. Additionally, we examined the expression levels of *TUBB3* and key molecules in the Akt/mTOR signaling pathway within the xenograft tissues. These experiments aimed to elucidate whether neuritin promotes GC progression at the organismal level, potentially providing a novel diagnostic and prognostic biomarker for GC.

Source of Funds:
Optimization and Clinical Promotion of the Best Therapeutic Protocol for SHPT Patients in the Perioperative Period (project no. KJGG202401, Shihezi University Research Program).

Data Availability Statement:
The data supporting the findings of this study are available from the corresponding author upon reasonable request.

Declaration of Interest:
The authors declared no competing interests for this work. All authors agreed to the submission and confirmed that the manuscript has not been published in whole or in parts nor that it has been submitted anywhere else.

References:

1. Smyth EC, Nilsson M, Grabsch HI, van Grieken NC, Lordick F. Gastric cancer. Lancet 2020 Aug 29;396(10251):635-48. (PMID: 32861308)

2. Tong W, Ye F, He L, et al. Serum biomarker panels for diagnosis of gastric cancer. Onco Targets Ther 2016 Apr 26;9:2455-63. (PMID: 27217769)

3. Morgan E, Arnold M, Camargo MC, et al. The current and future incidence and mortality of gastric cancer in 185 countries, 2020-40: A population-based modelling study. EClinicalMedicine 2022 Apr 21;47:101404. (PMID: 35497064)

4. Hooi JKY, Lai WY, Ng WK, et al. Global Prevalence of Helicobacter pylori Infection: Systematic Review and Meta-Analysis. Gastroenterology 2017 Aug;153(2):420-9. (PMID: 28456631)

5. Thrift AP, El-Serag HB. Burden of Gastric Cancer. Clin Gastroenterol Hepatol 2020 Mar;18(3):534-42. (PMID: 31362118)

6. Yu Z, Bai X, Zhou R, et al. Differences in the incidence and mortality of digestive cancer between Global Cancer Observatory 2020 and Global Burden of Disease 2019. Int J Cancer 2024 Feb 15;154(4):615-25. (PMID: 37750191)

7. Sung H, Ferlay J, Siegel RL, et al. Global Cancer Statistics 2020: GLOBOCAN Estimates of Incidence and Mortality Worldwide for 36 Cancers in 185 Countries. CA Cancer J Clin 2021 May; 71(3):209-49. (PMID: 33538338)

8. Sogutlu F, Pekerbas M, Biray Avci C. Epigenetic signatures in gastric cancer: current knowledge and future perspectives. Expert Rev Mol Diagn 2022 Dec;22(12):1063-75. (PMID: 36522183)

9. Joshi SS, Badgwell BD. Current treatment and recent progress in gastric cancer. CA Cancer J Clin 2021 May;71(3):264-79. (PMID: 33592120)

10. Roviello G, Polom K, Petrioli R, et al. Monoclonal antibodies-based treatment in gastric cancer: current status and future perspectives. Tumour Biol 2016 Jan;37(1):127-40. (PMID: 26566626)

11. Zhou S, Zhou J. Neuritin, a neurotrophic factor in nervous system physiology. Curr Med Chem 2014 Apr;21(10):1212-9. (PMID: 24350851)

12. Nedivi E, Hevroni D, Naot D, Israeli D, Citri Y. Numerous candidate plasticity-related genes revealed by differential cDNA cloning. Nature 1993 Jun 24;363(6431):718-22. (PMID: 8515813)

13. Zhao QR, Lu JM, Yao JJ, Zhang ZY, Ling C, Mei YA. Neuritin reverses deficits in murine novel object associative recognition memory caused by exposure to extremely low-frequency (50 Hz) electromagnetic fields. Sci Rep 2015 Jul 3;5:11768. (PMID: 26138388)

14. Naeve GS, Ramakrishnan M, Kramer R, Hevroni D, Citri Y, Theill LE. Neuritin: a gene induced by neural activity and neurotrophins that promotes neuritogenesis. Proc Natl Acad Sci U S A 1997 Mar 18;94(6):2648-53. (PMID: 9122250)

15. An K, Jung JH, Jeong AY, et al. Neuritin can normalize neural deficits of Alzheimer's disease. Cell Death Dis 2014 Nov 13; 5(11):e1523. (PMID: 25393479)

16. Dong H, Luo X, Niu Y, et al. Neuritin 1 expression in human normal tissues and its association with various human cancers. Int J Clin Exp Pathol 2018 Apr 1;11(4):1956-64. (PMID: 31938301)

17. Yuan M, Li Y, Zhong C, Li Y, Niu J, Gong J. Overexpression of neuritin in gastric cancer. Oncol Lett 2015 Dec;10(6):3832-6. (PMID: 26788217)

18. Schwanhäusser B, Busse D, Li N, et al. Global quantification of mammalian gene expression control. Nature 2011 May 19; 473(7347):337-42. (PMID: 21593866)

19. Wang ZY, Leushkin E, Liechti A, et al. Transcriptome and translatome co-evolution in mammals. Nature 2020 Dec;588(7839): 642-7. (PMID: 33177713)